www.nature.com/cr
www.cell-research.com

LETTER

Structural basis of acyl-CoA transport across the peroxisomal membrane by human ABCD1

Cell Research (2022) 32:214–217; https://doi.org/10.1038/s41422-021-00585-8

Dear Editor,

ABCD1, a member of the subfamily D of ABC transporters, participates in the transport of various fatty acid-CoA derivatives or very long-chain fatty acids (VLCFA) into the peroxisome and is essential for peroxisomal metabolism and lipid homeostasis.[1] Dysfunction of human ABCD1 is associated with neurodegenerative diseases, including X-linked adrenoleukodystrophy (X-ALD).[1] The molecular basis of substrate recognition and transport by human ABCD1 remains unknown. To date, four ABCD members have been identified in mammals.[1] As exporters, ABCD1–3 transport fatty acid-CoA derivatives or VLCFA from the cytosol into peroxisomes for β-oxidation with substrate preferences.[2] Their N-terminal regions, which is recognized by pEX19, play a role in facilitating the trafficking of ABCD1–3 to the peroxisome. In contrast, ABCD4 lacks this region, and functions as an importer to transport Vitamin B12 from the lysosome to the cytosol.[1] ABCD2, ABCD3 and ABCD4 display 65%, 40% and 28% sequence identity with ABCD1 (Supplementary information, Fig. S1). All ABCD transporters are half transporters and function as homodimers or heterodimers. With the exception of the structure of ATP-bound ABCD4,[3] no structural information is available about how the D family ABC transporters recognize and transport their substrates. Here, we report the structures of oleoyl-CoA-bound ABCD1 with the catalytic residue Glu630 in the nucleotide binding domain (NBD) substituted by glutamine ($ABCD1_{EQ}$) and ATP-bound $ABCD1_{EQ}$ (Fig. 1). Most recently, cryo-EM structures of ABCD1 in different conformations have also been reported in bioRxiv.[4–6]

The recombinant full-length human ABCD1 was expressed and purified from 293 GnTI$^-$ as described in Methods and Materials. The purified protein was stable and monodisperse as revealed by size exclusion chromatography (Supplementary information, Fig. S2a). We measured the ATPase activity of ABCD1 in digitonin solution. Since oleoyl-CoA is a potent substrate of ABCD1,[7] it was selected as a representative substrate. In absence of a substrate, both wild type ABCD1 ($ABCD1_{WT}$) and $ABCD1_{EQ}$ exhibit minimal baseline ATPase activity. In presence of the oleoyl-CoA, $ABCD1_{WT}$ exhibits a robust maximal ATPase activity (V_{max}) of about 214.6 nmol/min * mg, suggesting that binding of oleoyl-CoA robustly stimulates the basal ATPase activity of ABCD1 (Supplementary information, Fig. S2b). This observation is consistent with our studies of ABCG1.[8] The EQ mutant had been shown as a substitute of WT to determine the substrate bound conformation and to facilitate capturing the ATP bound state;[8,9] therefore, we prepared $ABCD1_{EQ}$ protein for structural determination. We determined cryo-EM structures of oleoyl-CoA-bound $ABCD1_{EQ}$ at 3.10 Å resolution (Supplementary information, Figs. S3, S4 and Table S1) and ATP-bound $ABCD1_{EQ}$ at 3.14 Å resolution (Supplementary information, Figs. S5, S6 and Table S1).

ABCD1 features a transmembrane domain (TMD) and a nucleotide binding domain (NBD) (Fig. 1a, b). Homodimeric ABCD1 exhibits a cytosol-facing conformation in the oleoyl-CoA bound state (Fig. 1a). The N-terminal residues 1–66, a loop region (residues 357–365), and the C-terminal residues 708–745 were not resolved. Additionally, the hinge region (residues 437–462) between TMD and NBD was invisible in the electron density probably due to flexibility. ABCD1 consists of 6 TM helices, with the TMD arrangement in the ABCD1 dimer displaying a similar pattern to B and C subfamily ABC transporters (Fig. 1a, b; Supplementary information, Fig S7).[10,11] The TM4 and TM5 helices of one protomer are intertwined with the TM1, TM2, TM3, and TM6 helices from another protomer, forming a V-shape cleft to bind substrate. Because a helix bridge has been observed between these two protomers, presumably to stabilize the dimer packing and to retain the proper cavity for accommodating substrates, we termed this helix Dimerized Helix (DH) (Fig. 1a, b).

In the cytosol-facing conformation of ABCD1, each protomer binds one oleoyl-CoA ligand (Fig. 1a). The oleoyl-CoA inserts deeply into the helix bundle embraced by TM3-TM6. The adenine moiety is locked in the cleft with the acyl chain of the oleoyl-CoA extending straight into the narrow cavity and exposed to the membrane boundary (Fig. 1a, c). Most residues participate in the specific recognition of oleoyl-CoA. The adenine moiety of oleoyl-CoA can be recognized by π–π stacking with Trp339 (Fig. 1c). The 3′ phosphate is stabilized by the formation of hydrogen bond with Ser340 and a salt bridge with Arg389. In addition, Ser226 and Ser244 form hydrogen bonds with the elongated pantetheine arm. Several residues such as Ile351, Ala354, and Leu377, make extensive hydrophobic contacts with the aliphatic tail (Fig. 1c). To validate our structure, we generated several ABCD1 variants, and detected the binding affinity using a fluorescence-based {N-[(7-nitro-2-1,3-benzoxadiazol-4-yl)-methyl]amino} (fNBD)-oleoyl-CoA binding assay. The fluorescence group attached to the aliphatic tail of oleoyl-CoA does not interfere with the binding. All related mutants, which were purified and exhibited good behavior in solution as $ABCD1_{EQ}$, abolished binding to varying degrees while $ABCD1_{EQ}$ exhibited binding equivalent to $ABCD1_{WT}$ (Fig. 1d). Importantly, mutations on the substrate recognition site (e.g., W339R, G343V, R389G and R389H), which have been deposited in the Human Gene Mutations Database (http://www.hgmd.cf.ac.uk), are implicated in neurodegenerative diseases.

The ATP-bound ABCD1 homodimer was determined at 3.14 Å resolution with C2 symmetry in a peroxisome-open conformation (Fig. 1a). The overall fold of ABCD1 is similar to that of ABCD4 with a root-mean-square deviation (RMSD) of 1.87 Å for 1037 Cα atoms (Fig. 1e). ATP is enclosed by Walker A, Walker B, Q loop, A loop, and the signature motif, making extensive contacts with the NBDs of the two protomers. The interaction details between ATP and $ABCD1_{EQ}$-NBD are shown in Fig. 1f. Quite a few disease-related mutations according to the Human Gene Mutations Database, including P484R, G507V, G512S, R518W and Q544R, are in the ATP

Received: 18 September 2021 Accepted: 18 October 2021
Published online: 9 November 2021

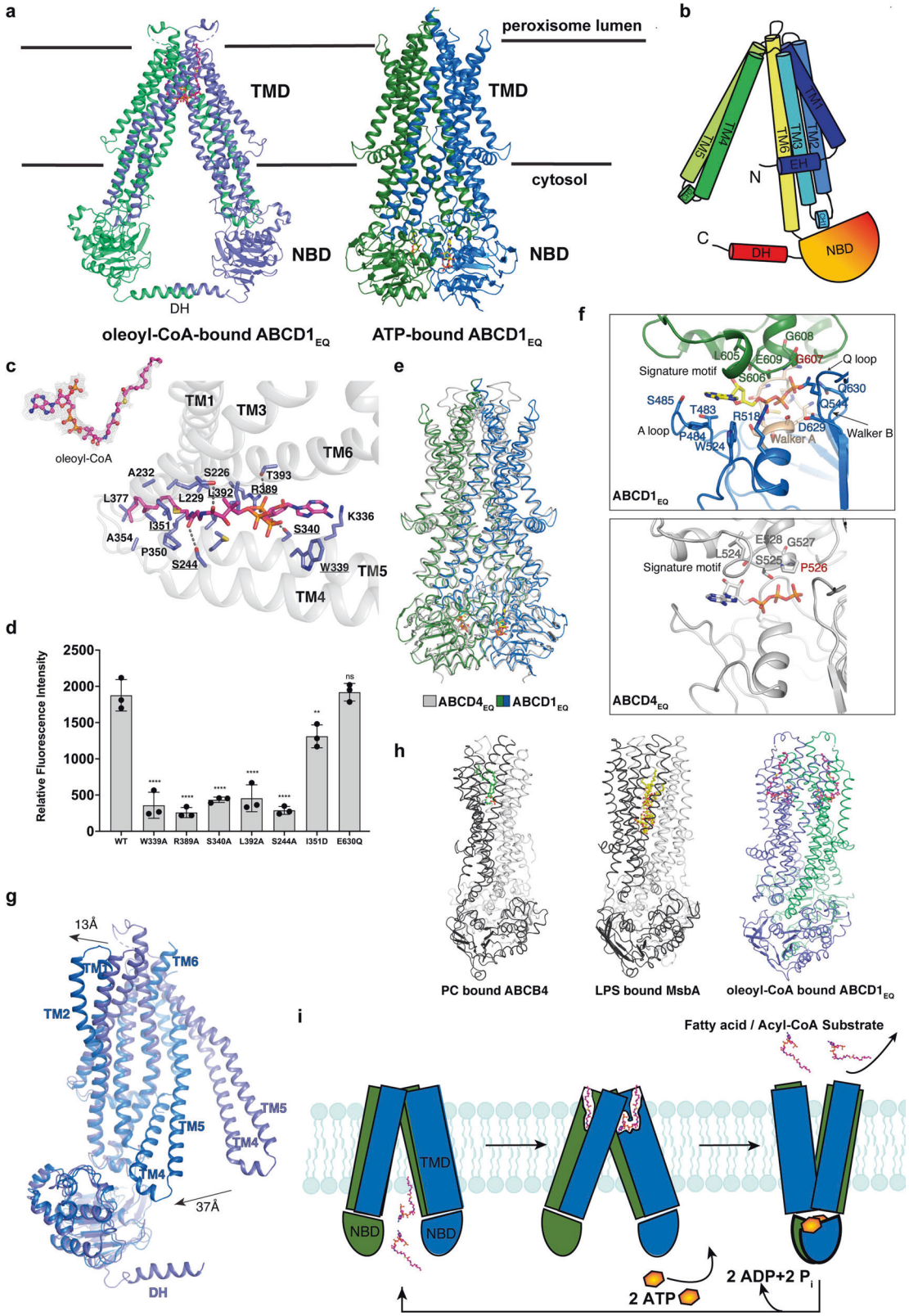

binding sites, indicating the clinical significance of ATP hydrolysis. Remarkably, the signature motif LSGGE of $ABCD1_{EQ}$ follows the canonical motif, which is different from the ABCD4 signature motif LSPGE (Fig. 1f).[3] When comparing the ATP- and oleoyl-CoA-bound $ABCD1_{EQ}$ structures, the DH region in the ATP-bound conformation is disordered, and the ATP-bound state presents a scissor-like motion along with a movement of ~37 Å by the interrupted TM4 and TM5 toward other helices (Fig. 1g). Concomitantly, a tilt of 13 Å by TM1–3 opens up a cavity, revealing ATP-mediated movements of the homodimers to shrink

Fig. 1 Cryo-EM structures of human ABCD1$_{EQ}$ in oleoyl-CoA-bound and ATP-bound conformations. a Overall structures of human ABCD1$_{EQ}$ in oleoyl-CoA- and ATP-bound conformations. Oleoyl-CoA and ATP are shown with magenta and yellow sticks. **b** Topology diagram for ABCD1 protomer. Secondary and key structural elements of TMD are indicated. **c** Interaction details of oleoyl-CoA and ABCD1$_{EQ}$. Cryo-EM map of oleoyl-CoA are shown at 3.5 σ level. Hydrogen bonds are labeled by dash lines, and residues that were validated by the binding assay are underlined. **d** The fNBD-oleoyl-CoA binding assay between WT or ABCD1 variants and fNBD-oleoyl-CoA. ****$P < 0.0001$, **$P < 0.001$. Data are means ± SD ($n = 3$). **e** Superposition of human ABCD1$_{EQ}$ and human ABCD4$_{EQ}$ (PDB: 6JBJ). ABCD1$_{EQ}$ is indicated same as (**a**), while ABCD4$_{EQ}$ is colored in gray. **f** Structural comparison of the ATP binding sites in ABCD1$_{EQ}$ and ABCD4$_{EQ}$. Walker A of ABCD1$_{EQ}$ is shown in wheat. Specific residues in the signature motif are highlighted in red. **g** Structural comparison of oleoyl-CoA-bound ABCD1$_{EQ}$ and ATP-bound ABCD1$_{EQ}$ protomers. Structural movements after ATP binding are indicated by black arrows. **h** ABCD1 employs a distinct recognition mechanism in comparison with ABCB4 (PDB: 7NIV) and MsbA (PDB: 5TV4). **i** A proposed model for acyl-CoA or fatty acids recruitment and transport by human ABCD1 in peroxisome. First, ABCD1 in the cytosol-facing conformation is ready to bind substrates, then two molecules of acyl-CoA or fatty acids can be recognized by one ABCD1 homodimer. ABCD1 will further undergo a dramatic conformational change when ATP is engaged by NBDs, leading to the release of these substrates to the peroxisome lumen. After ATP hydrolysis, ABCD1 returns to the resting state.

the cavity and release the substrates. Notably, an unknown extended density was observed in the exit of the cavity formed by TM3–6 helix bundle in each protomer, and the unknown molecule is surrounded by a hydrophobic area (Supplementary information, Fig. S8). This molecule may be a cholesteryl hemisuccinate (CHS) molecule that was introduced during the purification. Since it is unclear whether ABCD1 transports acyl-CoA as a CoA ester or free fatty acid across the peroxisomal membrane,[12] this molecule may also be free fatty acid. Further investigation is required to identify this molecule. A superposition was performed to compare these experimental structures of ABCD1$_{EQ}$ with the AlphaFold predicted protomer.[13] The oleoyl-CoA-bound ABCD1 fits well with the predicted protomer with exception to the large shift of the TM4–TM5 helices, while the ATP-bound ABCD1$_{EQ}$ superposes well with the predicted protomer besides a small movement of TM1, TM2 and TM6 (Supplementary information, Fig. S9). The experimental structures exhibit the physiological conformation ready to bind and release substrates compared with the AlphaFold predicted structure.

ABCD1 employs a distinct mechanism in comparison with other lipid-related ABC transporters. The lipid exporter ABCB4 which translocates phosphatidylcholine (PC) into bile canaliculi exhibits one binding pocket in the TMD region,[14] MsbA which flips lipopolysaccharide (LPS) from the cytoplasmic to the periplasmic leaflet also reveals a single LPS binding site in the interface of two protomers,[15] whereas ABCD1 show two acyl-CoA binding sites, suggesting a novel binding mode for the ABCD subfamily (Fig. 1h). Compared with the recently determined ABCD1 structures, the overall structures of ATP-bound state are similar.[5,6] In contrast, the nucleotide-free ABCD1 presents two distinct states according to the distance of two NBDs: one is akin to the state of our oleoyl-CoA-bound ABCD1 (open state); another is an intermediate state, which we did not observe, the distance of two NBDs is between that of the open state and ATP-bound ABCD1 (Fig. 1a). Moreover, the structure of C22:0-CoA bound ABCD1 reveals a different substrate-binding site that was generated by TMs 1, 3 and 6 and TMs 3-6 of another protomer in the intermediate state and the ATPase assay showed that mutations on this site could reduce the C22:0-CoA-stimulated ATPase activity.[6] It is possible that these findings may reveal alternative states of ABCD1 in the acyl-CoA transport cycle.

In summary, we determined cryo-EM structures of human ABCD1$_{EQ}$ in an oleoyl-CoA-bound cytosol-facing conformation and in an ATP-bound peroxisome-open conformation, demonstrating a distinct acyl-CoA recognition mechanism of the ABCD subfamily. These two different conformations of human ABCD1, along with the results of our binding assays, provide us with a mechanistic framework for understanding the transport mechanism of ABCD1. Two acyl-CoA molecules bind to the central cavity of the ABCD1 dimer, and ATP is engaged by the NBDs. After ATP hydrolysis, the resulting ADP molecules are released; at the same time, the acyl-CoA (or fatty acids if ABCD1 functions as an acyl-CoA thioesterase[12]) could be exported to the peroxisome lumen (Fig. 1i). Further investigations on ABCD members with various substrates will not only uncover more details of the molecular mechanisms of ABCD subfamily transporters, but also facilitate the potential treatment of related human diseases.

Rong Wang[1], Yu Qin[1] and Xiaochun Li[1,2]✉
[1]Department of Molecular Genetics, University of Texas Southwestern Medical Center, Dallas, TX, USA. [2]Department of Biophysics, University of Texas Southwestern Medical Center, Dallas, TX, USA.
✉email: xiaochun.li@utsouthwestern.edu

DATA AVAILABILITY

The 3D cryo-EM density map of oleoyl-CoA-bound and ATP-bound structures of ABCD1$_{EQ}$ have been deposited in the Electron Microscopy Data Bank under the accession numbers EMD-25131 and EMD-25130. Atomic coordinate for the atomic model of oleoyl-CoA-bound and ATP-bound structures of ABCD1$_{EQ}$ have been deposited in the Protein Data Bank under the accession numbers 7SHN and 7SHM. All other data are available from the corresponding authors upon reasonable request.

REFERENCES

1. Kawaguchi, K. & Morita, M. *Biomed. Res. Int.* **2016**, 6786245 (2016).
2. Hlavac, V. & Soucek, P. *Biochem. Soc. Trans.* **43**, 937–942 (2015).
3. Xu, D. et al. *Cell Res.* **29**, 1039–1041 (2019).
4. Jia, Y. et al. *bioRxiv*, https://doi.org/10.1101/2021.09.24.461756 (2021).
5. My Le, L. T. et al. *bioRxiv*, https://doi.org/10.1101/2021.09.04.458904 (2021).
6. Chen, Z.-P. et al. *bioRxiv*, https://doi.org/10.1101/2021.09.24.461565 (2021).
7. van Roermund, C. W. et al. *FASEB J.* **22**, 4201–4208 (2008).
8. Sun, Y. et al. *Proc. Natl. Acad. Sci. USA* **118** (2021).
9. Manolaridis, I. et al. *Nature* **563**, 426–430 (2018).
10. Song, G. et al. *Cell Discov.* **7**, 55 (2021).
11. Johnson, Z. L. & Chen, J. *Cell* **172**, 81–89 (2018).
12. Kawaguchi, K. et al. *Sci.Rep.* **11**, 2192 (2021).
13. Jumper, J. et al. *Nature* **596**, 583–589 (2021).
14. Nosol, K. et al. *Proc. Natl. Acad. Sci. USA* **118**, https://doi.org/10.1073/pnas.2106702118 (2021).
15. Mi, W. et al. *Nature* **549**, 233–237 (2017).

ACKNOWLEDGEMENTS

We thank Y. Sun and D. Stoddard for assistance in data collection and E. Debler for editing paper. This work was supported by NIH grants P01HL020948, R01GM135343 and Welch Foundation (I-1957) (to X.L.). X.L. is a Damon Runyon-Rachleff Innovator supported by the Damon Runyon Cancer Research Foundation (Grant DRR-53S-19) and a Rita C. and William P. Clements Jr. Scholar in Biomedical Research at UT Southwestern Medical Center.

AUTHOR CONTRIBUTIONS

R.W. and Y.Q. purified the protein. R.W. carried out cryo-EM work and performed the biochemical study. All the authors analyzed the data and contributed to paper preparation. R.W. and X.L. wrote the paper.

COMPETING INTERESTS

The authors declare no competing interests.

ADDITIONAL INFORMATION

Supplementary information The online version contains supplementary material available at https://doi.org/10.1038/s41422-021-00585-8.

Correspondence and requests for materials should be addressed to Xiaochun Li.